

## Research Article

# Interaction of Pulses of Different Duration with Chemically Prepared Silver Nanoparticles: Analysis of Optical Nonlinearities

Ke Zhang,<sup>1,2</sup> Rashid A. Ganeev ,<sup>1</sup> Konda Srinivasa Rao,<sup>1</sup> Sandeep Kumar Maurya,<sup>1</sup> Ganjaboy S. Boltaev,<sup>1</sup> P. S. Krishnendu,<sup>1</sup> Zhi Yu,<sup>1</sup> Weili Yu,<sup>1</sup> Yue Fu,<sup>1,2</sup> and Chunlei Guo <sup>1,3</sup>

<sup>1</sup>The Guo China-US Photonics Laboratory, State Key Laboratory of Applied Optics, Changchun Institute of Optics, Fine Mechanics and Physics, Chinese Academy of Sciences, Changchun 130033, China

<sup>2</sup>University of Chinese Academy of Sciences, Beijing 100049, China

<sup>3</sup>The Institute of Optics, University of Rochester, Rochester NY 14627, USA

Correspondence should be addressed to Rashid A. Ganeev; rashid\_ganeev@mail.ru and Chunlei Guo; guo@optics.rochester.edu

Received 2 August 2018; Accepted 23 December 2018; Published 31 January 2019

Academic Editor: Giuseppe Compagnini

Copyright © 2019 Ke Zhang et al. This is an open access article distributed under the Creative Commons Attribution License, which permits unrestricted use, distribution, and reproduction in any medium, provided the original work is properly cited.

The nonlinear optical properties of the aqueous solutions of silver nanoparticles (Ag NPs) prepared by chemical reduction method are analyzed using femtosecond and picosecond pulses at different wavelengths. In the case of 800 and 400 nm, the growths of nonlinear absorption and nonlinear refraction with the increase of Ag NP concentration, as well as a change at the signs of nonlinear optical processes, are determined. The nonlinear absorption coefficient and nonlinear refractive index of Ag NP solutions measured using picosecond pulses were a few orders of magnitude larger than those in the case of femtosecond probe pulses. We also demonstrate the optical limiting properties of Ag NPs using 800 nm, 60 fs pulses.

## 1. Introduction

Metal nanoparticles (NPs) have unique properties allowing applications in mechanics, catalysis, magnetism, optics, electricity, new material development, and heat physics, due to their morphology and size effects [1–5]. Among them, noble metal NPs have potential applications in the field of nanophotonics due to their strong nonlinear optical response, thus attracting significant attention [4–8]. As a typical representative of noble metals, silver nanoparticles (Ag NPs) are particularly prominent [9–16]. Silver nanoparticles have attracted large attention previously due to a possibility in converting ultrafine silver nanoclusters to monodisperse silver sulfide nanoparticles [11], advanced performance of silver nanoparticles in the catalysis of the oxygen reduction reaction in neutral media [13], newly developed methods of diagnosis of breast cancer by surface-enhanced Raman spectroscopy of silver nanoparticles [14], enhanced antibacterial activity of bifunctional Fe<sub>3</sub>O<sub>4</sub>-Ag core-shell nanostructures [16], etc. Alongside the morphological properties, the optical

and nonlinear optical features of these small dimensional structures became the subject of numerous studies.

The analysis of the nonlinear absorption coefficients and nonlinear refractive indices of Ag NPs, as well as the exploration of their potential applications, was reported in a few studies [17–19]. There are experimental studies showing that particle size, morphology, and surrounding medium of noble metal NPs have great influence on their nonlinear optical properties [20–23]. For example, Ag NPs with smaller particle sizes demonstrated weak nonlinear optical response, while larger particles were characterized by strong saturable absorption (SA) [20]. With the increase of particle sizes, nonlinear absorption has shown a shift from two-photon absorption (2PA) to SA, while nonlinear refraction was transformed from self-defocusing to self-focusing [21]. The SA caused by the ground state bleaching can lead to decrease of absorption in the sample. At the same time, the change of incident intensity of a probe laser pulse can also cause the variation of nonlinear optical properties, such as the shift from SA to reverse saturable absorption (RSA) [24, 25]. As the incident intensity

increases, the RSA leads to enhancement of nonlinear absorption in the sample.

The collective oscillation of free electrons in Ag NPs results in the appearance of a strong surface plasmon resonance (SPR) at  $\sim 410$  nm. The characteristic absorption peak of SPR in the visible band, fast time response, and large nonlinear optical properties make Ag NPs attractive for research and applications in optical communication, optical storage, optical switch, polarization sensitive photodetectors, and nonlinear optics [14, 21, 26]. Previous research on the nonlinear optical properties of Ag NPs was mainly focused on the influence of incident intensity on their characteristics. There is a number of studies which show that Ag NPs demonstrate SA at low pulse intensity, while at higher intensities, the RSA becomes a dominating process. There are also a few reports on the variations of optical nonlinearities at different morphologies of Ag NPs [22, 23]. However, to the best of our knowledge, there are no systematic studies reported on the optical limitation, the influence of different concentrations of Ag NPs in liquids, and the effects of laser pulse duration, wavelength, and repetition rate on their nonlinear optical properties.

In this paper, we analyze the nonlinear absorption and nonlinear refraction of Ag NP aqueous solutions of different concentrations, which were prepared by chemical reduction method. Z-scan measurements at different pulse durations (40 fs, 200 ps, and, in some cases, 5 ns) and wavelengths (800, 400, and 355 nm) are presented. We analyze the influence of different pulse repetition rates on the nonlinear optical characteristics. Additionally, we present our optical limiting and pump-probe studies of these NP solutions.

## 2. Experimental Arrangements

**2.1. Preparation and Characterization of Ag NPs.** Ag NPs were synthesized by a chemical reduction of silver nitrate ( $\text{AgNO}_3$ ) and sodium borohydride ( $\text{NaBH}_4$ ). 0.043 g of  $\text{AgNO}_3$  was dissolved in 50 mL deionized water, and 0.012 g of  $\text{NaBH}_4$  was dissolved in 150 mL of deionized water. The obtained  $\text{NaBH}_4$  solution was placed under the condition of an ice water bath ( $0^\circ\text{C}$ ) and stirred quickly. The  $\text{AgNO}_3$  solution was trickled slowly and evenly into the  $\text{NaBH}_4$  solution, allowing it to react fully under the ice water bath. With the addition of  $\text{AgNO}_3$ , the solution gradually turned yellow, indicating that Ag NPs are formed. Ag NPs with different concentrations were obtained by adding different amounts of  $\text{AgNO}_3$  solution.

The absorption spectra of prepared Ag NP solutions were measured by the UV-visible spectrophotometer (Cary Series, Agilent Technologies). The absorption spectra of solutions at the two concentrations are shown in Figure 1(a), which demonstrates the SPR absorption peaks at around 400 nm. In the case of the UV-visible spectral measurements, we used the 10 mm thick quartz cells. Therefore, at 400 nm probe radiation, we observed the high absorbance of the cell containing larger concentration of Ag nanoparticles. We did not use these cells for Z-scans due to large absorbance at 400 nm and long length of medium, which exceeds the Rayleigh length of the focused beam. In the latter case, the

conventional relations of Z-scans are not applicable for the fitting procedure, while in the former case, one can meet with the problem of the validity of the Z-scan formalism and approximations at high absorbance. Because of these two reasons, we used the 2 mm thick fused silica cells for our Z-scan studies, to exclude the problems of the validity of our Z-scans. In that case, the absorbance at the SPR of Ag nanoparticles became equal at 1.1 instead of 2.5 in the case of the 10 mm thick cell.

The intensities of absorption peaks were proportional to the concentrations of NPs. The morphology and particle size of Ag NPs were measured by a scanning electron microscope (SEM) (S-4800, Hitachi). The NPs exhibited a regular spherical structure (Figure 1(b)). The particle size distribution lay between 7 and 20 nm, with mean size of 13 nm.

To calculate the Ag NP concentration, we followed the method reported in Ref. [27]. It was assumed that Ag atoms form the spherical NPs with a close packing of the surface core. The volume of Ag atoms in the particles was estimated to be 74%, and the particle size of Ag NPs was calculated to be 13 nm. From these data, the concentrations ( $C$ ) of the two solutions of Ag NPs were calculated to be  $1.5 \times 10^{-9}$  and  $4.7 \times 10^{-9}$  mol/L.

NP suspensions were periodically tested during the two-month period of these studies. Absorption spectroscopy and SEM analysis showed that basic characteristics, such as SPR peak, particle sizes, and morphology, remain stable.

**2.2. Z-Scan, Pump Probe, and Optical Limiting Schemes.** The Ti:Sapphire laser (Spitfire Ace, Spectra-Physics) was used in these studies. It provided the 60 fs pulses at a wavelength of 800 nm and a repetition rate of 1 kHz. 10% of the output from the regenerative amplifier of this laser was separated prior to the compressor stage from the main beam and used in different stages of these studies. The duration of these uncompressed pulses (200 ps) was measured by a homemade autocorrelator. To study the effect of different wavelengths of probe pulses on the nonlinear optical characteristics of Ag NPs, the barium borate (BBO) crystal was used to convert 800 nm radiation to its second harmonic ( $\lambda = 400$  nm).

Figure 2 shows the experimental setups for the Z-scan, pump probe, and optical limiting studies, respectively. The standard single-beam Z-scan scheme [28] was used for the measurements of the nonlinear optical properties of NPs (Figure 2(a)) using picosecond and femtosecond pulses. The laser pulse was focused by a lens with a focal length of 400 mm, and then, the radiation transmitted through the sample was measured by power meter or photodiode. The full widths at half maximum and  $1/e^2$  maximum of intensity distribution of the 800 nm radiation at the focal plane were measured to be 42 and 76  $\mu\text{m}$ , respectively. The aperture in front of the registrar was fully opened in the case of the open-aperture (OA) scheme. The nonlinear absorption coefficient ( $\beta$ ) of Ag NPs was calculated from the OA Z-scan curve. To obtain closed-aperture (CA) Z-scan, the aperture was partially closed to allow 10% of incident energy to pass through towards the photodiode. The CA Z-scan curve allowed the determination of both  $\beta$  and nonlinear refractive index ( $\gamma$ ) of the analyzed Ag NP solution. Before the Z-scan

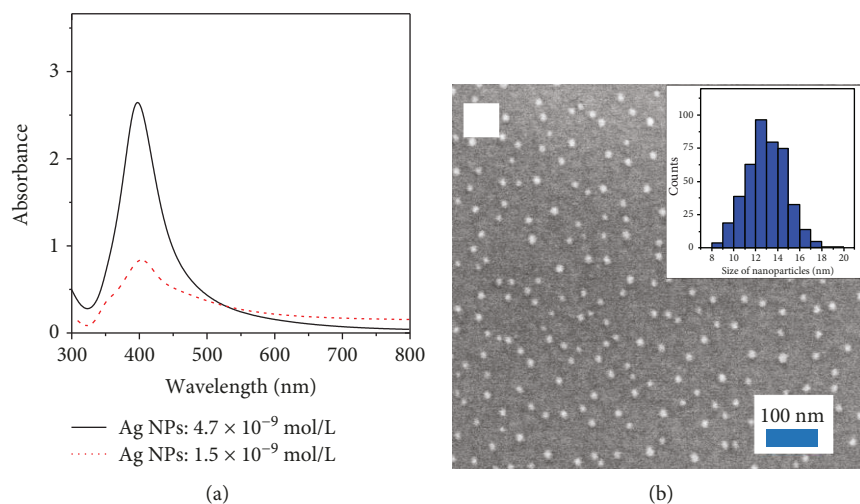


FIGURE 1: (a) UV-visible absorption spectra of the two Ag NP solutions of different concentrations. (b) SEM image of Ag NPs and corresponding size distribution.

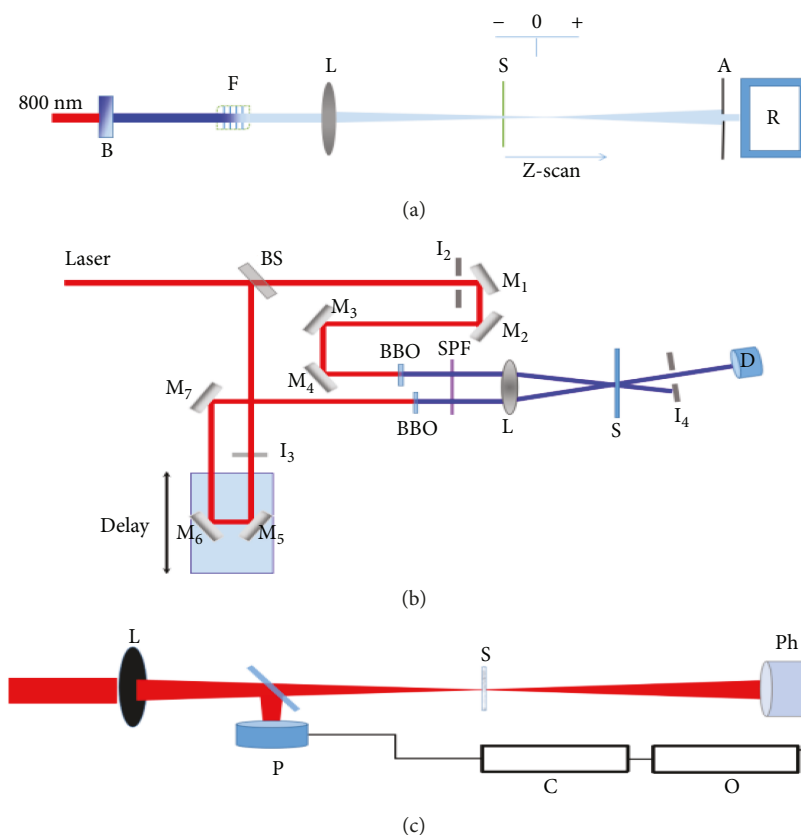


FIGURE 2: Experiment layouts for the (a) Z-scan, (b) pump probe, and (c) optical limiting studies. (a) B: barium borate crystal (BBO); F: filters; L: lens,  $f = 400$  mm; S: sample; A: aperture; R: recording device. (b) BS: beam splitter; M: mirrors; L: lens,  $f = 400$  mm; I: iris apertures; BBO: barium borate crystal; D: detector; SPF: short pass filter; S: sample. (c) L: lens,  $f = 400$  mm; P: power meter; S: sample; C: computer; O: oscilloscope; Ph: photodiode.

measurements, we analyzed the spatial characteristics of probe beams using a CCD camera (Thorlabs) and confirmed that the beam profiles in the focal area were close to Gaussian, which is a prerequisite for the analysis of Z-scan traces using the relations developed for this technique.

The transient absorption (TA) measurements of Ag NP solutions were carried out by the pump-probe technique using 400 nm, 60 fs pulses. The laser pulse from the amplifier was split in the ratio of 30:70 with the use of a beam splitter. The transmitted beam was used as a pump pulse,

and the reflected beam was used as a probe pulse (Figure 2(b)). The probe pulse passed through the pair of mirrors mounted on a motorized translating stage, which served as a time delay control between pump and probe pulses. A 2 mm thick BBO crystal was used to generate the 400 nm pulses for our experiments. Pump and probe pulses were focused on the 2 mm fused silica cell containing the Ag NP solution using 300 mm focal length lens. The energy and beam waist ratios of pump and probe pulses at focus were adjusted to be 10:1 and 1:2, respectively, to match the conditions required for TA. The zero time delay for pump and probe pulses was determined using the 0.2 mm thick type-I BBO crystal at the sample position using two 800 nm beams. Time delay between pump and probe pulses was controlled using the motorized translating stage. Ultrafast photodiode was used to measure the transmittance of the probe pulse through the sample with respect to the sample's position, which was further converted to the time units. The mixed domain oscilloscope (MDO3054, Tektronix) was used for the acquisition of a photodiode signal with respect to the translation stage driven by the motion controller (EPS 301, Newport).

In the case of optical-limiting experiments, the samples were installed in the focal plane (Figure 2(c)). We gradually increased the energy of the 800 nm, 60 fs pulses and analyzed a decrease of transmittance of the cells filled with low ( $1.5 \times 10^{-9}$  mol/L) and high ( $4.7 \times 10^{-9}$  mol/L) concentrations of Ag NPs.

### 3. Results

**3.1. Nonlinear Optical Relations of Z-Scans.** The low and high concentration Ag NP solutions were prepared by similar chemical method. Therefore, they had the same particle size and shape. Their morphology is shown in Figure 1(b). The SEM image presents a uniform structure of spherical NPs with the particle size distribution centered at 13 nm (see inset in Figure 1(b)). In these experiments, we used laser pulses of different durations to conduct the OA and CA Z-scans of these Ag NP solutions. Studies were performed at 800 and 400 nm wavelengths using picosecond and femtosecond pulses.

For the OA Z-scan curve, the following formula was used for the fitting with experimental data [28]:

$$T(z) = \sum_{m=0}^{\infty} \frac{(-q)^m}{(m+1)^{3/2}} \approx 1 - \frac{q}{2\sqrt{2}}, \quad q = \frac{\beta I_0 L_{\text{eff}}}{1 + z^2/z_0^2}. \quad (1)$$

Here,  $\beta$  is the nonlinear absorption coefficient determined in SI units;  $L_{\text{eff}} = [1 - \exp(-\alpha_0 L)]/\alpha_0$  is the effective length of the medium;  $\alpha_0$  is the linear absorption coefficient;  $L$  is the thickness of our samples;  $z_0$  is the Rayleigh length;  $z_0 = k(w_0)^2/2$ ,  $k = 2\pi/\lambda$ , is the wave number;  $w_0$  is the beam waist radius at the  $1/e^2$  level of intensity distribution; and  $I_0$  is the laser radiation intensity in the focal plane. By defining from fitting the value of  $q_0 = \beta I_0 L_{\text{eff}}$  at focal plane ( $z = 0$ ), one can find the nonlinear absorption coefficient  $\beta = q_0/I_0 L_{\text{eff}}$ .

The formula used for SA fitting is [29]

$$T(z) = 1 + \frac{I_0}{I_{\text{sat}} \times (1 + z^2/z_0^2)}. \quad (2)$$

Here,  $I_{\text{sat}}$  is the saturation intensity, which depends on the concentration of the Ag NPs in the solution, the effective cross-sections of nonlinear optical processes, and the relaxation time constants. This parameter indicates the intensity at which the transmittance of the sample increases two times due to the bleaching.

For the CA Z-scan curve, the following formula was used for the process of nonlinear refraction and absorption [30]:

$$T(z) = 1 + \frac{2(-\rho x^2 + 2x - 3\rho)}{(x^2 + 9)(x^2 + 1)} \Delta\Phi_0, \quad (3)$$

where  $x = z/z_0$ ,  $\rho = \beta/2k\gamma$ ,  $\Delta\Phi_0 = k\gamma I_0 L_{\text{eff}}$ , and  $\Delta\Phi_0$  is the phase change due to nonlinear refraction. The corresponding nonlinear refractive index can be obtained using the relation  $\gamma = \Delta\Phi_0/kI_0 L_{\text{eff}}$ . Then,  $\beta$  can be calculated from the  $\rho$  determined using the fitting procedure.

Before these experiments, the fused silica cell containing deionized water was tested by the Z-scan at different pulse energies. In that case, we did not observe any nonlinear optical absorption and refraction. Meanwhile, the nonlinear optical response of the aqueous suspension containing Ag nanoparticles was observed even at low pulse energy. Therefore, it was concluded that the nonlinear optical refraction and absorption of studied colloidal suspension can be attributed solely to the silver nanoparticles.

**3.2. Z-Scan Measurements Using Picosecond Pulses.** In this subsection, the 200 ps pulses were used for the OA and CA Z-scans in the aqueous solutions of Ag NPs. The experimental results in the off-resonant case (800 nm) using 200 ps pulses are shown in Figure 3. The theoretical fitting of experimental results was carried out, and these curves are shown in the corresponding figures.

The intensity of  $I = 6 \times 10^7 \text{ W cm}^{-2}$  was used in the case of low concentration Ag NP aqueous solution and OA Z-scan (Figure 3(c)). This Z-scan curve shows the influence of 2PA. The nonlinear absorption coefficient was calculated to be  $2 \times 10^{-8} \text{ cm W}^{-1}$ . At a higher concentration of Ag NPs, the incident intensity was reduced by 15 times to  $0.4 \times 10^7 \text{ W cm}^{-2}$ . The nonlinear absorption in that case was also induced by 2PA, while the nonlinear absorption coefficient was increased by 15 times ( $\beta = 3 \times 10^{-7} \text{ cm W}^{-1}$ , Figure 3(d)) compared with that of a low concentration. The growth of the nonlinear absorption coefficient is mainly caused by the increase of the concentration. It was shown that the influence of the concentration of NPs in the solution on the nonlinear absorption coefficient is far greater than that of the incident intensity. The comparison of the nonlinear refractive indices of the aqueous solutions of Ag NPs at the two different concentrations measured using the CA Z-scan leads to similar conclusion. In the case of CA Z-scans, we reduced the incident

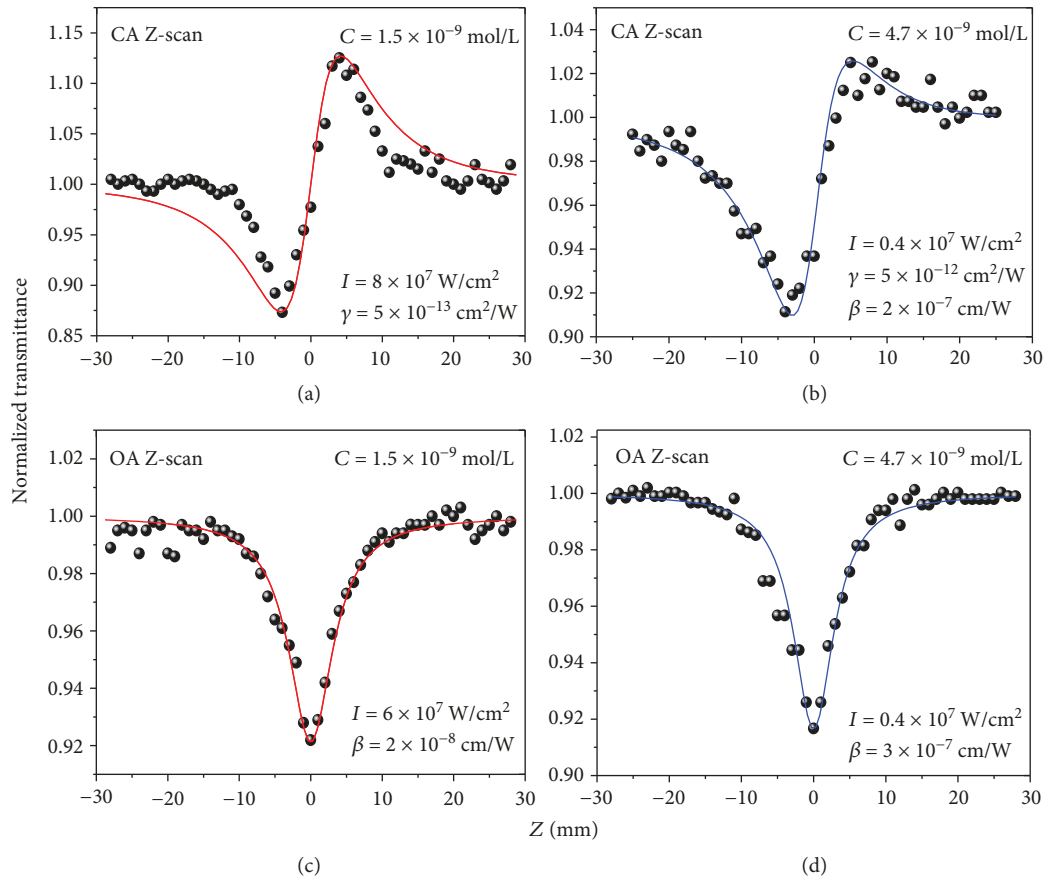


FIGURE 3: Experimental results (spheres) and theoretical fittings (solid curves) of CA (a, b) and OA (c, d) Z-scans of the Ag NP solutions of different concentrations ( $C = 1.5 \times 10^{-9}$  mol/L (a, c),  $C = 4.7 \times 10^{-9}$  mol/L (b, d)) using 800 nm, 200 ps laser pulses.

intensity from the  $8 \times 10^7$  W cm<sup>-2</sup> at a low concentration to  $0.4 \times 10^7$  W cm<sup>-2</sup> at a high concentration, while the nonlinear refractive index in the latter case was increased by 10 times ( $\gamma = 5 \times 10^{-13}$  and  $5 \times 10^{-12}$  cm<sup>2</sup>W<sup>-1</sup> in the cases shown in Figures 3(a) and 3(b), respectively). Thus, the nonlinear refractive index notably rises with the increase of the concentration. Notice that measurements of  $\beta$  and  $\gamma$  of the same sample at different intensities resulted in similar values, which point out the insignificant influence of laser intensities on these parameters at used experimental conditions.

CA Z-scan in the case of a higher concentration of NPs also allowed the determination of  $\beta$  using the fitting of Eq. (3) with experimental data (Figure 3(b)). The calculated value of  $\beta$  in that case ( $2 \times 10^{-7}$  cm W<sup>-1</sup>) was close to the one measured using the OA Z-scan ( $3 \times 10^{-7}$  cm W<sup>-1</sup>, Figure 3(d)). We found  $\beta$  of the Ag NP solution from the known  $\gamma$ , which was determined from the fitting of CA experimental data, and  $\rho$ . Since any step in this procedure provides some systematic errors, the determination of nonlinear absorption coefficient by this method becomes less accurate, compared with the direct method of fitting the OA Z-scan data. Thus, smaller uncertainty in the calculation of  $\beta$  arises from a single-step procedure including the fitting of the OA Z-scan curve.

In the case of 400 nm, 200 ps pulses, the OA and CA Z-scans were similarly performed using the two concentrations

of NPs. The experimental results and theoretical fittings are shown in Figure 4. The same intensity in the focal plane ( $1 \times 10^7$  W cm<sup>-2</sup>) was used for the two concentrations during these OA and CA Z-scans. In the case of the OA Z-scans, RSA was the main mechanism of nonlinear absorption at different concentrations of NPs. At the conditions of a higher concentration, the nonlinear absorption coefficient was two times larger compared to the low concentration case ( $\beta = 1 \times 10^{-7}$  and  $2 \times 10^{-7}$  cm W<sup>-1</sup>, Figures 4(c) and 4(d), respectively). The threefold growth of the nonlinear refractive index for these two concentrations was observed ( $6 \times 10^{-13}$  and  $2 \times 10^{-12}$  cm<sup>2</sup>W<sup>-1</sup>, Figures 4(a) and 4(b), respectively).

The increase of the NP concentration obviously enhanced the nonlinear optical characteristics of the studied solution at  $\lambda = 400$  nm. However, there was not much of a significant change in nonlinear optical parameters compared with those of the 800 nm probe pulses. The nonlinear optical characteristics of the NPs of the same concentration at different wavelengths were compared and analyzed, and the results are as follows. In the case of low concentration, even at significantly (6 to 8 times) reduced intensity in the focal plane, the nonlinear absorption coefficient and nonlinear refractive index measured at  $\lambda = 400$  nm were higher than those measured at the 800 nm wavelength. The same was also observed at higher concentration conditions.

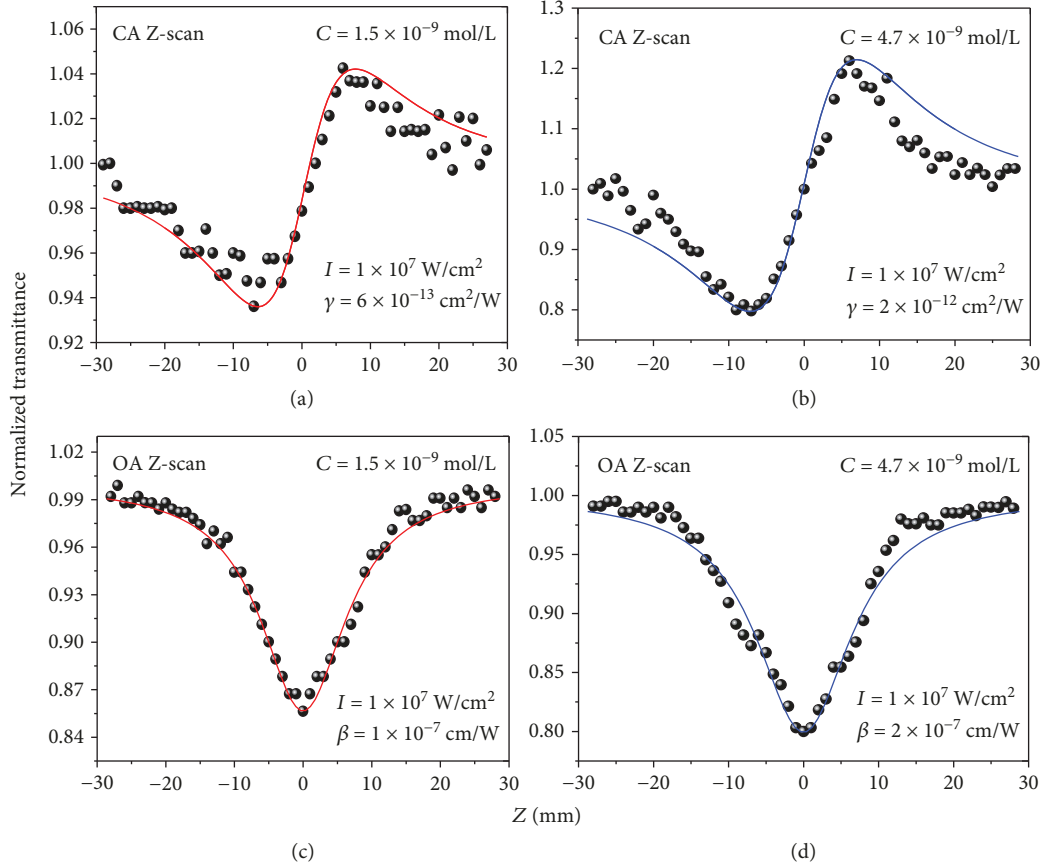


FIGURE 4: Experimental results and theoretical fittings of CA and OA Z-scans of the Ag NP solutions of different concentrations using 400 nm, 200 ps laser pulses.

**3.3. Z-Scan Measurements Using Femtosecond Pulses.** The experimental results and theoretical fittings of OA and the CA Z-scan using 800 nm, 60 fs pulses at the two concentrations of NPs are shown in Figure 5. At these conditions, we observed a significant decrease of the nonlinear optical characteristics compared with the case of using 200 ps probe pulses. The calculated data of  $\beta$  and  $\gamma$  are presented on the graphs.

Under the same incident intensity ( $2 \times 10^{11} \text{ W cm}^{-2}$ ), the increase of the concentration led to a considerable growth of the nonlinear absorption coefficient and nonlinear refractive index, similar to the experiments using picosecond pulses. The growth rate of the nonlinear refractive index was approximately the same as that of the concentration ( $\gamma = 3 \times 10^{-16}$  and  $1 \times 10^{-15} \text{ cm}^2 \text{ W}^{-1}$ , Figures 5(a) and 5(b), respectively). In the meantime, the nonlinear absorption coefficient was increased from  $1.5 \times 10^{-12}$  to  $7 \times 10^{-12} \text{ cm W}^{-1}$ , i.e., almost 5 times, with the threefold growth of the NP concentration (Figures 5(c) and 5(d), respectively).

The experimental results and theoretical fittings of the OA and CA Z-scans using shorter wavelength femtosecond pulses (400 nm, 60 fs) are shown in Figure 6. Under these conditions, the OA and CA Z-scan curves were completely different from those observed in the case of 800 nm picosecond and femtosecond pulses, as well as 400 nm picosecond pulses. The OA Z-scans at the two different concentrations

of NPs showed the SA (Figures 6(a) and 6(b)). The threefold growth of the concentration caused the twofold increase of the negative nonlinear absorption coefficient ( $-4 \times 10^{-11}$  and  $-8 \times 10^{-11} \text{ cm W}^{-1}$ , Figures 6(c) and 6(d), respectively). The saturation intensities were calculated to be  $2 \times 10^{11}$  and  $9 \times 10^{10} \text{ W cm}^{-2}$  for the low and high concentrations of Ag NPs.

The CA Z-scan curves showed the self-defocusing in our samples (Figures 6(a) and 6(b)). Similarly, the growth of the NP concentration led to the increase of the nonlinear refractive index ( $-8 \times 10^{-16}$  and  $-4 \times 10^{-15} \text{ cm}^2 \text{ W}^{-1}$ ). The analysis of experimental results using femtosecond pulses at the same concentration shows that, at off-resonant conditions ( $\lambda = 800 \text{ nm}$ ), the nonlinear absorption was attributed to 2PA, while in the resonant case ( $\lambda = 400 \text{ nm}$ ), it was caused by SA. The nonlinear refraction correspondingly transforms from the self-focusing in the case of the abovementioned measurements (Figures 3–5) to the self-defocusing in the case of 400 nm, 60 fs probe pulses. This peculiarity was maintained at both low and high concentrations of NPs.

We also used the low pulse repetition rate (50 Hz) of femtosecond pulses to carry out Z-scans in the aqueous solutions of Ag NPs at the two concentrations. The studies showed that, at  $\lambda = 800 \text{ nm}$ , no difference between the Z-scans at the low and high pulse repetition rates was observed.

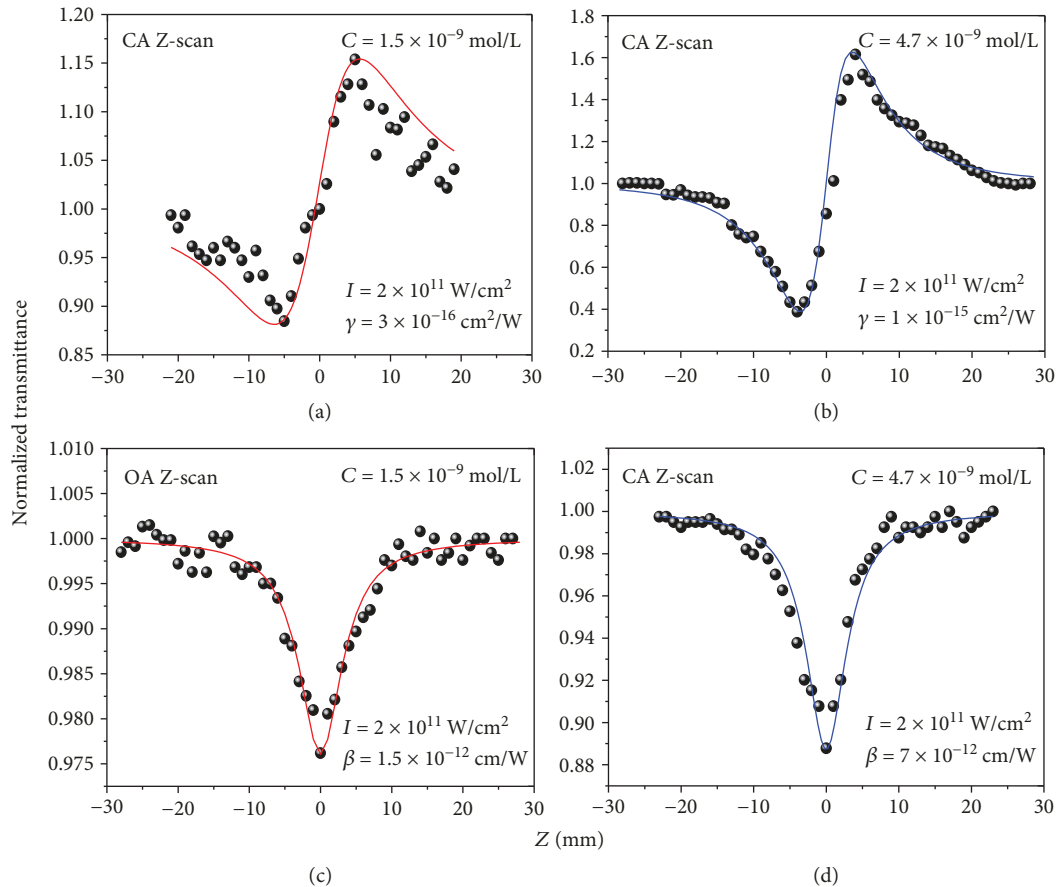


FIGURE 5: Experimental results and theoretical fittings of CA and OA Z-scans of the Ag NP solutions of different concentrations using 800 nm, 60 fs pulses.

Similarly, at the 400 nm wavelength of femtosecond pulses, the CA Z-scans of lower and higher concentrations of Ag NPs showed self-defocusing in the case of 50 and 1000 Hz pulse repetition rates. These studies at different pulse repetition rates confirmed the absence of a thermal lens and its influence on the appearance of negative nonlinear refraction. As deduced from the spectral measurements, the absorption at 400 nm was not high to induce the thermal effects at the used cell thickness (2 mm). At these conditions, the accumulation of heat even at a 1 kHz repetition rate did not cause the appearance of the negative lens. That is why the calculated nonlinear refractive indices in the two cases of Z-scans (i.e., at 1 kHz and 50 Hz) did not show a measurable difference.

In general, under the condition of a 1 kHz pulse repetition rate at the 800 nm laser wavelength, the application of picosecond radiation led to 2PA at different concentrations. In the meantime, there is a lot of studies showing that at a shorter wavelength, the incident intensity affects the nonlinear absorption coefficient (for example, [31]). The growth of incident intensity in the Ag NP solution causes transformation from SA to RSA [11, 26, 32]. There is an intensity threshold between SA and RSA. At some conditions, the nonlinear absorption coefficient also increases with the growth of laser intensity [26, 32].

In our case, there was a large difference in the case of the nonlinear optical parameters of NP solutions measured by picosecond and femtosecond pulses. At off-resonant conditions ( $\lambda = 800$  nm, 60 fs),  $\beta$  and  $\gamma$  were positive, while at resonant conditions ( $\lambda = 400$  nm, 60 fs), they were negative. At the same concentration, the nonlinear absorption coefficient in the case of 800 nm picosecond probe pulses was four orders of magnitude larger than that measured using femtosecond pulses. At resonance conditions ( $\lambda = 400$  nm), this ratio was also equal to four orders of magnitude. For the nonlinear refractive indices, the results obtained using picosecond pulses were approximately three orders of magnitude larger than those measured using femtosecond probe pulses.

In addition, the third harmonic of the Nd:YAG nanosecond laser was used in this study. The OA Z-scan experiments using 355 nm, 5 ns, 10 Hz repetition rate pulses were carried out on the aqueous solution containing a high concentration of Ag NPs under different incident intensities. The sample at these conditions showed SA, and the growth of incident intensity led to the enhancement of positive nonlinear absorption leading to the prevailing dominance of RSA.

The large difference in the nonlinearities of NPs can be caused by the involvement of various nonlinear optical processes. In particular, the role of saturable and reverse saturable absorption can be largely enhanced at the conditions

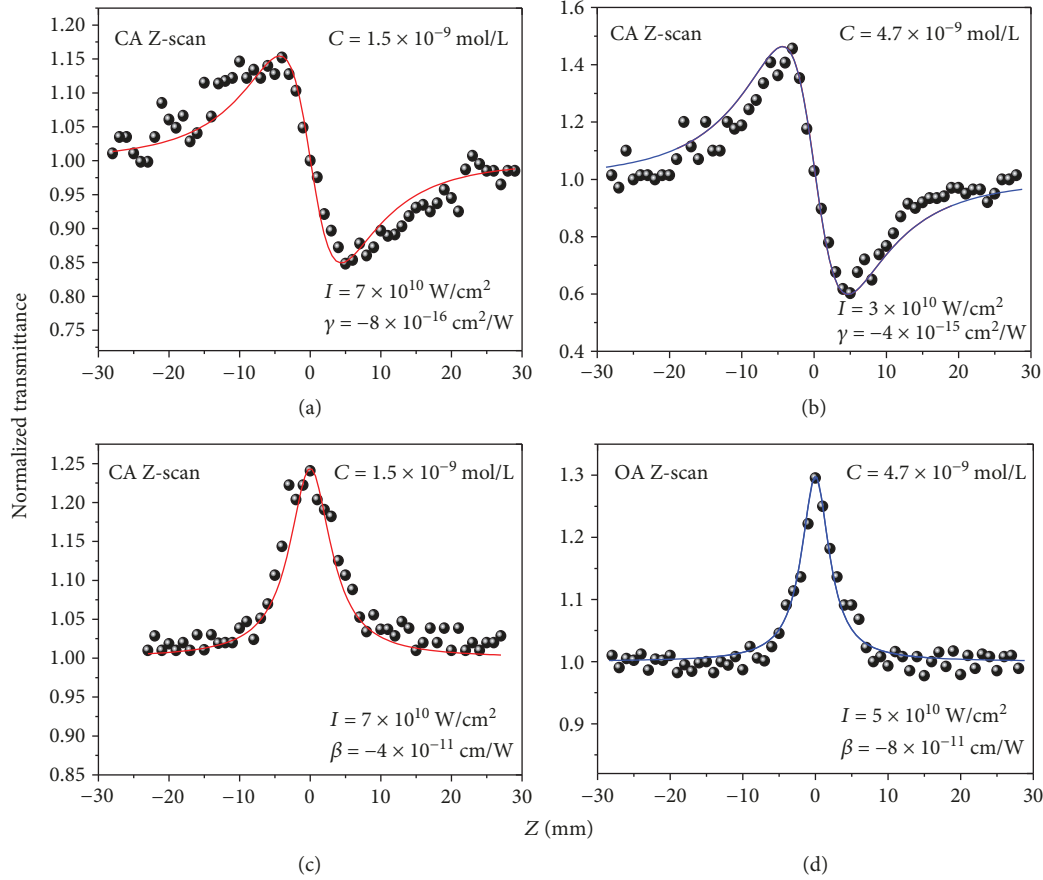


FIGURE 6: Experimental results and theoretical fittings of CA and OA Z-scans of the Ag NP solutions of different concentrations using 400 nm, 60 fs pulses.

when the relaxation time constants of excited states participating in those processes become larger compared with short laser pulses. At those conditions, longer (picosecond) probe pulses can cause larger nonlinear optical response compared with femtosecond pulses. To determine the relaxation time constants, we carried out the pump-probe transient absorption studies on our samples.

**3.4. Pump-Probe Measurements of Transient Absorption.** TA measurements for chemically synthesized Ag NPs ( $C = 4.7 \times 10^{-9}$  mol/L) were performed using noncollinear degenerate pump-probe spectroscopy using 400 nm, 60 fs pulses. Figure 7 represents the TA profile of Ag NPs in deionized water measured using the femtosecond pump pulse fluence of  $25 \mu\text{J}/\text{cm}^2$ . Prior to the TA study of Ag NP, the TA profile for water was also measured, which showed no change in the transmittance of the probe pulse at the maximum fluence used in this experiment ( $100 \mu\text{J}/\text{cm}^2$ ). TA profile was compared with the single exponential fit to determine the relaxation time constant, which was measured to be  $\tau_1 = 3.9$  ps at the pump pulse fluence of  $25 \mu\text{J}/\text{cm}^2$ . This parameter is significantly larger compared with the pulse duration using femtosecond pulses. In the case of Ag NPs, excitation generally happens through plasmon excitation where the electron-electron-scattering time scale is of the order of a few femtoseconds, whereas the electron-phonon interaction

lasts much longer with the time scale of a few picoseconds [33]. The femtosecond dynamics associated with the electron-electron scattering in Ag NPs was not observed in the TA profile, which can be explained by faster electron-electron-scattering dynamics compared to the employed laser pulse width [33, 34]. The electron-phonon interaction in Ag NPs generally occurs in the 100 fs to ps time scale; hence, the time constant of 3.9 ps can directly be attributed to the electron-phonon interaction at 400 nm.

TA profiles for Ag NPs at higher pump pulse fluences demonstrated the variation of transient bleaching at 400 nm. Figure 8 shows the influence of pump pulse fluence on the TA profile of Ag NPs. It was observed that the transmittance of the probe pulses increased beyond 10 ps with the increase of pump pulse fluence. We found from Figure 8 that the threshold for the transient bleaching of the synthesized Ag NPs was at about  $46 \mu\text{J}/\text{cm}^2$ , which is lower than the data reported in Ref. [34]. This change in transmittance occurs due to a significantly higher electron temperature. This leads to the energy transfer to the surrounding solvent through phonon-phonon coupling [35, 36]. Another possible reason for the increase of the transmittance beyond 10 ps can be the heat flow from Ag NPs to the surrounding water, which results in the decrease of the optical dielectric constant with the growth of the temperature of water beyond  $100^\circ\text{C}$  [37]. Thus, the change in

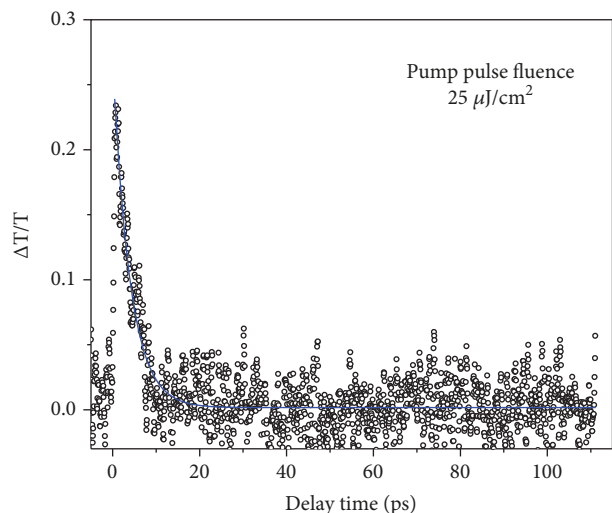


FIGURE 7: Transient absorption profile with respect to delay time in the case of 400 nm laser pulses. Scattered empty circles show the experimental measurements, and the solid line represents the single exponential fit to the experimental data.

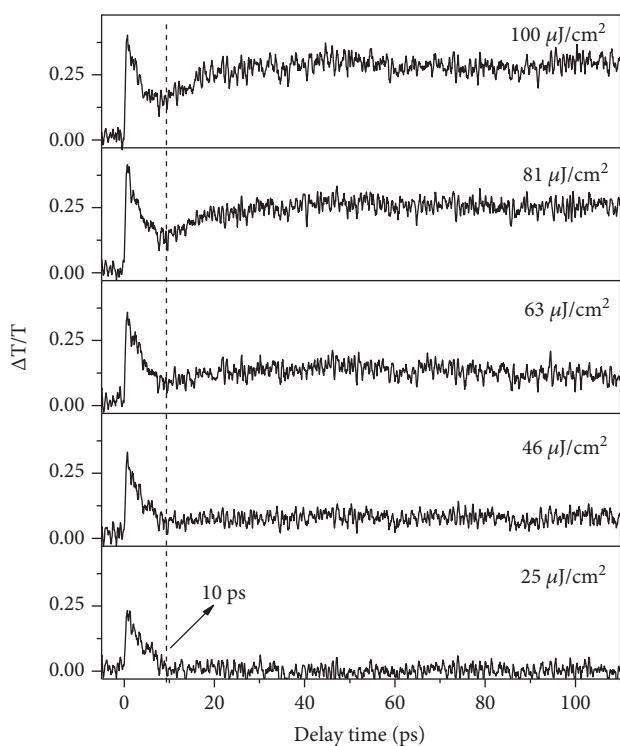


FIGURE 8: Transient absorption profiles with respect to delay time for chemically prepared Ag NPs ( $C = 4.7 \times 10^{-9}$  mol/L) at varying pump pulse fluences of femtosecond 400 nm pulses.

the transmittance beyond 10 ps also supports the strong coupling between phonon modes of the nanoparticle and the surrounding water.

**3.5. Optical Limiting in Ag NP Solutions.** Optical limiting is generally analyzed using nanosecond pulses. Meanwhile, femtosecond pulses can effectively avoid heat accumulation

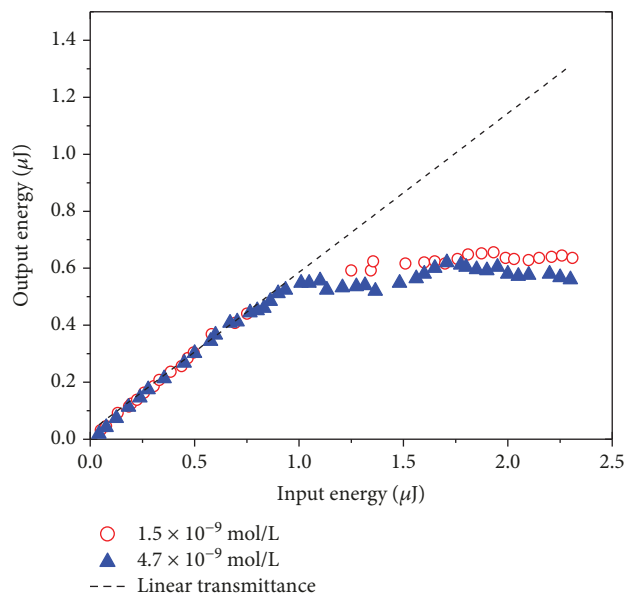


FIGURE 9: Optical limiting of 800 nm, 60 fs pulses using Ag NP solutions at low ( $C = 1.5 \times 10^{-9}$  mol/L, empty circles) and high ( $C = 4.7 \times 10^{-9}$  mol/L, filled triangles) concentrations.

and other effects compared with nanosecond pulses. Below, we present our studies of this process using femtosecond pulses. Figure 9 demonstrates the optical limiting in the Ag NP solutions at the two concentrations in the case of 800 nm, 60 fs radiation. As it is shown in the figure, the transmitted energy increases linearly with the growth of the incident pulse energy in the low energy range and then reaches the saturation.

When the incident energy of 800 nm pulses increased above  $0.75 \mu\text{J}$ , the transmitted energy tends to approach a steady value. The optical limiting threshold was defined as the maximum transmitted energies  $E_{\text{OL}} = \sim 0.5 \mu\text{J}$  and  $E_{\text{OL}} = \sim 0.6 \mu\text{J}$  in the case of high and low concentrations of NPs, respectively. One can see that this parameter decreases with the growth of Ag NP concentration.

## 4. Discussion and Conclusions

All measured nonlinear optical parameters are collected in Table 1, where we show the  $\gamma$ ,  $\beta_{2\text{PA}}$ ,  $\beta_{\text{RSA}}$ ,  $\beta_{\text{SA}}$ ,  $I_{\text{sat}}$ ,  $\tau_1$ , and  $E_{\text{OL}}$  for the two concentrations of NPs and two wavelengths (800 and 400 nm).

The studies of the nonlinear optical properties of Ag NPs at different experimental conditions have already been reported. However, all of them were carried out using the limiting range of variations of the temporal characteristics of probe pulses.

Here, we presented a systematical study of these species using pulse spanning from femtosecond to nanosecond time scale. Based on these studies, we showed the advantages of using picosecond pulses, which cause the largest nonlinear optical response in Ag NPs.

The origin of nonlinearity in the case of NPs is the change in the frequency of localized surface plasmon resonance

TABLE 1: Nonlinear optical parameters of Ag NP solutions.

	$C = 1.5 \times 10^{-9}$ mol/L				$C = 4.7 \times 10^{-9}$ mol/L			
	800 nm		400 nm		800 nm		400 nm	
	ps	fs	ps	fs	ps	fs	ps	fs
$\gamma$ ( $\text{cm}^2 \text{W}^{-1}$ )	$5 \times 10^{-13}$	$3 \times 10^{-16}$	$6 \times 10^{-13}$	$-8 \times 10^{-16}$	$5 \times 10^{-12}$	$1 \times 10^{-15}$	$2 \times 10^{-12}$	$-4 \times 10^{-15}$
$\beta_{2\text{PA}}$ ( $\text{cm W}^{-1}$ )	$2 \times 10^{-8}$		$1 \times 10^{-7}$		$3 \times 10^{-7}$		$2 \times 10^{-7}$	
$\beta_{\text{RSA}}$ ( $\text{cm W}^{-1}$ )		$1.5 \times 10^{-12}$				$7 \times 10^{-12}$		
$\beta_{\text{SA}}$ ( $\text{cm W}^{-1}$ )				$-4 \times 10^{-11}$				$-8 \times 10^{-11}$
$I_{\text{sat}}$ ( $\text{W cm}^{-2}$ )				$2 \times 10^{11}$				$9 \times 10^{10}$
$\tau_1$ (ps)								3.9
$E_{\text{OL}}$ ( $\mu\text{J}$ )		0.6				0.5		

caused by the change in the electron temperature. These nonlinearities are realized in the forms of 2PA, SA, and RSA.

The results of pump-probe studies in metal nanoparticles show that nonlinearities measured using pulses shorter than the thermalization time for electrons (pulse width less than 300 fs) would be weak. The TA explains our observations of the nonlinear properties of NPs. It causes SA, which may further transform towards RSA.

In this paper, we have systematically analyzed the optical, structural, and nonlinear optical properties of 13 nm silver nanoparticles using probe pulses of different durations. The nonlinear optical properties of Ag NP aqueous solutions prepared by chemical reduction method under the different conditions were compared using the single-beam Z-scan technique. The experimental results show that nonlinear absorption coefficient and nonlinear refractive index are strongly dependent on the NP concentration in the solutions and the duration of probe pulses. In the case of picosecond probe pulses, the nonlinear absorption coefficient of Ag NPs at off-resonant conditions ( $\lambda = 800$  nm) was four orders of magnitude larger than that in the case of femtosecond probe pulses. In the resonance case ( $\lambda = 400$  nm), this ratio was also equal to four orders of magnitude.

For the nonlinear refractive indices, this value was approximately three orders of magnitude higher once compared to the studies using picosecond and femtosecond probe pulses. OA Z-scans were also carried out close to the resonance band of Ag NPs at the high concentration of the Ag NP aqueous solution under the conditions of application of the nanosecond pulses ( $\lambda = 355$  nm). At different incident energies, the OA Z-scans showed the SA overpassed by RSA with the growth of laser pulse energy. The high and low pulse repetition rates were used for Z-scans to show that the repetition rate has no significant effect on the nonlinear optical characteristics of our samples at used experimental conditions. In addition, the recovery time of these nonlinear processes was measured by a degenerate pump-probe transient absorption technique using 400 nm radiation ( $\tau_1 = 3.9$  ps). The effect of bleaching was observed with the increase of pump pulse fluence above  $46 \mu\text{J}/\text{cm}^2$ , which occurs beyond the 10 ps time scale. Finally, we have demonstrated the optical limiting of Ag NPs using 800 nm, 60 fs pulses, which showed the twofold decrease of propagated pulses at  $E = 2.25 \mu\text{J}$  of

incident radiation and stabilization of the optical limiting at the  $E = 0.5\text{-}0.6 \mu\text{J}$  of output pulses.

Recently, the nonlinear optical studies of the Ag NPs prepared by another method, i.e., during ablation of bulk silver in water using different wavelengths and durations of heating pulses, were reported [38]. The joint appearance of nonlinear optical refraction and absorption was analyzed using the 1064 nm, 5 ns and 800 nm, 60 fs probe pulses. The highest nonlinear absorption coefficient of ablation-induced Ag NPs was  $3.0 \times 10^{-5} \text{ cm W}^{-1}$  at the wavelength of 1064 nm in the case of 5 ns probe pulses. This value was calculated taking into account the  $10^{-3}$  volume part of the nanoparticles synthesized during laser ablation of silver in water and assuming the local field factor of  $10^{-2}$  taking into account the quantum confinement effect of nanoparticles in the suspension. Notice that in our case, we present the nonlinear absorption coefficient of the suspension (not a single NP), which was just two orders of magnitude smaller ( $3 \times 10^{-7} \text{ cm W}^{-1}$ ) than the one of Ag NPs reported in Ref. [38]. It means that once we assume the similar volume part of chemically prepared NPs in our suspension ( $10^{-3}$ ), the NP nonlinear absorption coefficient will surpass the one in the case of ablation-produced silver nanoparticles.

## Data Availability

The data of these studies are not available either in archives or in separate folders in the Internet, since those are only collected during experiments and kept in our computers. The data used to support the findings of this study are available from the corresponding author upon request.

## Conflicts of Interest

The authors declare that they have no conflicts of interest.

## Acknowledgments

The financial support from the Natural Science Foundation of China (61774155 and 61705227) and the National Key Research and Development Program of China (2017YFB1104700) is appreciated. R.A.G. thanks the Chinese Academy of Sciences President's International

Fellowship Initiative (Grant No. 2018VSA0001) for the financial support.

## References

- [1] C. Lu, X. Hu, K. Shi et al., “An actively ultrafast tunable giant slow-light effect in ultrathin nonlinear metasurfaces,” *Light: Science & Applications*, vol. 4, article e302, 2015.
- [2] F. Chen, J. Cheng, S. Dai, and Q. Nie, “Z-scan and optical Kerr shutter studies of silver nanoparticles embedded bismuthate glasses,” *Journal of Non-Crystalline Solids*, vol. 377, pp. 151–154, 2013.
- [3] T. Karali, N. Can, L. Valberg et al., “Optical properties and luminescence of metallic nanoclusters in ZnO:Cu,” *Physica B Condensed Matter*, vol. 363, no. 1-4, pp. 88–95, 2005.
- [4] Y. H. Su, Y. F. Ke, S. L. Cai, and Q. Y. Yao, “Surface plasmon resonance of layer-by-layer gold nanoparticles induced photoelectric current in environmentally-friendly plasmon-sensitized solar cell,” *Light: Science & Applications*, vol. 1, no. 6, article e14, 2012.
- [5] M. Anija, J. Thomas, N. Singh et al., “Nonlinear light transmission through oxide-protected Au and Ag nanoparticles: an investigation in the nanosecond domain,” *Chemical Physics Letters*, vol. 380, no. 1-2, pp. 223–229, 2003.
- [6] O. Blum and N. T. Shaked, “Prediction of photothermal phase signatures from arbitrary plasmonic nanoparticles and experimental verification,” *Light: Science & Applications*, vol. 4, article e322, 2015.
- [7] J. T. Seo, Q. Yang, W.-J. Kim et al., “Optical nonlinearities of Au nanoparticles and Au/Ag coreshells,” *Optics Letters*, vol. 34, no. 3, pp. 307–309, 2009.
- [8] T. Jia, T. He, P. Li, Y. Mo, and Y. Cui, “A study of the thermal-induced nonlinearity of Au and Ag colloids prepared by the chemical reaction method,” *Optics and Laser Technology*, vol. 40, no. 7, pp. 936–940, 2008.
- [9] R. A. Ganeev, M. Baba, A. I. Rysanyansky, M. Suzuki, and H. Kuroda, “Characterization of optical and nonlinear optical properties of silver nanoparticles prepared by laser ablation in various liquids,” *Optics Communication*, vol. 240, no. 4-6, pp. 437–448, 2004.
- [10] R. A. Ganeev, A. I. Rysanyansky, A. L. Stepanov, and T. Usmanov, “Saturated absorption and nonlinear refraction of silicate glasses doped with silver nanoparticles at 532 nm,” *Optical and Quantum Electronics*, vol. 36, no. 10, pp. 949–960, 2004.
- [11] Y. Feng, Q. Yao, J. Li, N. Goswami, J. Xie, and J. Yang, “Converting ultrafine silver nanoclusters to monodisperse silver sulfide nanoparticles via a reversible phase transfer protocol,” *Nano Research*, vol. 9, no. 4, pp. 942–950, 2016.
- [12] Y. Gao, W. Wu, D. Kong, L. Ran, Q. Chang, and H. Ye, “Femtosecond nonlinear absorption of Ag nanoparticles at surface plasmon resonance,” *Physica E: Low-dimensional Systems and Nanostructures*, vol. 45, pp. 162–165, 2012.
- [13] C. C. M. Neumann, E. Laborda, K. Tschulik, K. R. Ward, and R. G. Compton, “Performance of silver nanoparticles in the catalysis of the oxygen reduction reaction in neutral media: efficiency limitation due to hydrogen peroxide escape,” *Nano Research*, vol. 6, no. 7, pp. 511–524, 2013.
- [14] A. Hernández-Arteaga, J. de Jesús Zermeño Nava, E. S. Kolosovas-Machuca et al., “Diagnosis of breast cancer by analysis of sialic acid concentrations in human saliva by surface-enhanced Raman spectroscopy of silver nanoparticles,” *Nano Research*, vol. 10, no. 11, pp. 3662–3670, 2017.
- [15] T. Yamamoto, K. Machi, S. Nagare, K. Hamada, and M. Senna, “The relation between surface plasmon resonance and morphology of Ag nanodots prepared by pulsed laser deposition,” *Solid State Ionics*, vol. 172, no. 1-4, pp. 299–302, 2004.
- [16] K. Tschulik, B. Haddou, D. Omanović, N. V. Rees, and R. G. Compton, “Coulometric sizing of nanoparticles: cathodic and anodic impact experiments open two independent routes to electrochemical sizing of Fe<sub>3</sub>O<sub>4</sub> nanoparticles,” *Nano Research*, vol. 6, no. 11, pp. 836–841, 2013.
- [17] R. A. Ganeev, “Nonlinear refraction and nonlinear absorption of various media,” *Journal of Optics A: Pure and Applied Optics*, vol. 7, no. 12, pp. 717–733, 2005.
- [18] R. A. Ganeev, A. I. Rysanyansky, S. R. Kamalov, M. K. Kodirov, and T. Usmanov, “Nonlinear susceptibilities, absorption coefficients and refractive indices of colloidal metals,” *Journal of Physics D*, vol. 34, no. 11, pp. 1602–1611, 2001.
- [19] G. Krishna Podagatlapalli, S. Hamad, S. P. Tewari, S. Sreedhar, M. D. Prasad, and S. Venugopal Rao, “Silver nano-entities through ultrafast double ablation in aqueous media for surface enhanced Raman scattering and photonics applications,” *Journal of Applied Physics*, vol. 113, article 073106, 2013.
- [20] G. H. Fan, S. L. Qu, Z. Y. Guo, Q. Wang, and Z. G. Li, “Size-dependent nonlinear absorption and refraction of Ag nanoparticles excited by femtosecond lasers,” *Chinese Physics B*, vol. 21, no. 4, article 047804, 2012.
- [21] P. Lu, K. Wang, H. Long, M. Fu, and G. Yang, “Size-related third-order optical nonlinearities of Au nanoparticle arrays,” *Optics Express*, vol. 18, 2010.
- [22] J. Jayabalan, A. Singh, R. Chari, and S. M. Oak, “Ultrafast third-order nonlinearity of silver nanospheres and nanodiscs,” *Nanotechnology*, vol. 18, no. 31, 2007.
- [23] C. Zheng, W. Li, W. Chen, and X. Ye, “Nonlinear optical behavior of silver nanopentagons,” *Materials Letters*, vol. 116, pp. 1–4, 2014.
- [24] B. H. Yu, D. L. Zhang, Y. B. Li, and Q. B. Tang, “Nonlinear optical behaviors in a silver nanoparticle array at different wavelengths,” *Chinese Physics B*, vol. 22, no. 1, article 014212, 2013.
- [25] A. Ajami, W. Husinsky, B. Svecova, S. Vytykacova, and P. Nekvindova, “Saturable absorption of silver nanoparticles in glass for femtosecond laser pulses at 400 nm,” *Journal of Non-Crystalline Solids*, vol. 426, pp. 159–163, 2015.
- [26] U. Gurudas, E. Brooks, D. M. Bubb, S. Heiroth, T. Lippert, and A. Wokaun, “Saturable and reverse saturable absorption in silver nanodots at 532 nm using picosecond laser pulses,” *Journal of Applied Physics*, vol. 104, no. 7, article 073107, 2008.
- [27] S. Xingcan, Q. Yuan, H. Liang, H. Yan, and X. He, “Hysteresis effects of the interaction between serum albumins and silver nanoparticles,” *Science in China Series B: Chemistry*, vol. 46, no. 4, pp. 387–398, 2003.
- [28] M. Sheik-Bahae, A. A. Said, T. H. Wei, D. J. Hagan, and E. W. van Stryland, “Sensitive measurement of optical nonlinearities using a single beam,” *IEEE Journal of Quantum Electronics*, vol. 26, no. 4, pp. 760–769, 1990.
- [29] P. B. Chapple, J. Staromlynska, J. A. Hermann, T. J. McKay, and R. G. Mcduff, “Single-beam Z-scan: measurement techniques and analysis,” *Journal of Nonlinear Optical Physics & Materials*, vol. 6, no. 3, pp. 251–293, 1997.

- [30] X. Liu, S. Guo, H. Wang, and L. Hou, "Theoretical study on the closed-aperture Z-scan curves in the materials with nonlinear refraction and strong nonlinear absorption," *Optics Communication*, vol. 197, no. 4-6, pp. 431–437, 2001.
- [31] K. Wang, J. Zhou, L. Yuan et al., "Anisotropic third-order optical nonlinearity of a single ZnO micro/nanowire," *Nano Letters*, vol. 12, no. 2, pp. 833–838, 2012.
- [32] M. Hari, S. Mathew, B. Nithyaja, S. A. Joseph, V. P. N. Nampoori, and P. Radhakrishnan, "Saturable and reverse saturable absorption in aqueous silver nanoparticles at off-resonant wavelength," *Optical and Quantum Electronics*, vol. 43, no. 1-5, pp. 49–58, 2012.
- [33] J.-Y. Bigot, V. Halte, J.-C. Merle, and A. Daunois, "Electron dynamics in metallic nanoparticles," *Chemical Physics*, vol. 251, no. 1-3, pp. 181–203, 2000.
- [34] J. H. Hodak, I. Martini, and G. V. Hartland, "Spectroscopy and dynamics of nanometer-sized noble metal particles," *The Journal of Physical Chemistry B*, vol. 102, no. 36, pp. 6958–6967, 1998.
- [35] T. S. Ahmadi, S. L. Logunov, and M. A. El-Sayed, "Picosecond dynamics of colloidal gold nanoparticles," *The Journal of Physical Chemistry*, vol. 100, no. 20, pp. 8053–8056, 1996.
- [36] S. L. Logunov, T. S. Ahmadi, M. A. El-Sayed, J. T. Khoury, and R. L. Whetten, "Electron dynamics of passivated gold nanocrystals probed by subpicosecond transient absorption spectroscopy," *The Journal of Physical Chemistry B*, vol. 101, no. 19, pp. 3713–3719, 1997.
- [37] D. Eisenberg and W. Kaurzmann, *The Structure and Properties of Water*, Oxford University Press, New York, Ny, USA, 1969.
- [38] G. S. Boltaev, R. A. Ganeev, P. S. Krishnendu et al., "Strong third-order optical nonlinearities of Ag nanoparticles synthesized by laser ablation of bulk silver in water and air," *Applied Physics A: Materials Science & Processing*, vol. 124, no. 11, p. 766, 2018.



**Hindawi**  
Submit your manuscripts at  
[www.hindawi.com](http://www.hindawi.com)

